Original Article

Manufacturing of Si-W-O Nanorods via Hydrothermal Synthesis for Methylene Blue Removal from Aqueous Solution

Abdullah A. Faqihi[1]

[1]Department of Industrial Engineering, College of Engineering and Computer Sciences, Jazan University, Jazan 45142, Saudi Arabia

Abstract

This study presents the hydrothermal manufacturing, structural characterization, and evaluation of the adsorption performance of silicon–tungsten oxide (Si–W–O) nanorods as engineered functional materials for methylene blue removal from aqueous solutions. Emphasis is placed on the process–structure–performance relationship governing adsorption behavior. The hydrothermal manufacturing route enabled the controlled formation of crystalline Si–W–O nanorods with a uniform rod-like morphology and accessible surface sites, leading to enhanced adsorption performance. Structural and morphological analyses indicated the successful formation of the Si–W–O nanorods, highlighting the strong relationship between the manufacturing process, structural characteristics, and adsorption performance.

Batch adsorption experiments demonstrated rapid adsorption behavior, with significant methylene blue removal occurring within the first 15 min before equilibrium was reached. At a low dye concentration (25 ppm), the manufactured nanorods achieved near-complete removal efficiency (≈95–100%), while higher concentrations (100 ppm) led to reduced efficiency (~63%) due to active site saturation. Increasing material loading from 10 to 50 mg significantly improved removal performance from ~35% to ~98%, demonstrating the beneficial effect of increasing adsorbent loading.

Process conditions, including pH, ionic strength, and temperature, strongly influenced adsorption performance. Optimal removal efficiency (~98%) was achieved within a pH range of 3–7, while elevated ionic strength and temperature reduced removal efficiency, suggesting that the adsorption process may involve electrostatic interactions and exhibit predominantly exothermic behavior. FTIR analysis suggested interactions between methylene blue molecules and oxygen-containing surface groups on the Si–W–O nanorods.

A possible adsorption mechanism involves a synergistic combination of electrostatic attraction, hydrogen bonding, and surface complexation. From a manufacturing engineering perspective, the hydrothermally manufactured Si–W–O nanorods represent a promising class of functional nanomaterials for potential wastewater treatment applications owing to their controllable manufacturing route, favorable morphology, and excellent adsorption performance.

Keywords: Hydrothermal Manufacturing**;** Methylene Blue Removal; Hydrothermal Treatment; Adsorption Mechanism.

Address for correspondence:
E-mail: afaqihi@jazanu.edu.sa,
https://orcid.org/0009-0006-3512-9850
Received: 10.05.2026; **Revision:** 19.05.2026; **Accepted:** 20.07.2026; **Published:** 13.08.2026

Graphical abstract:

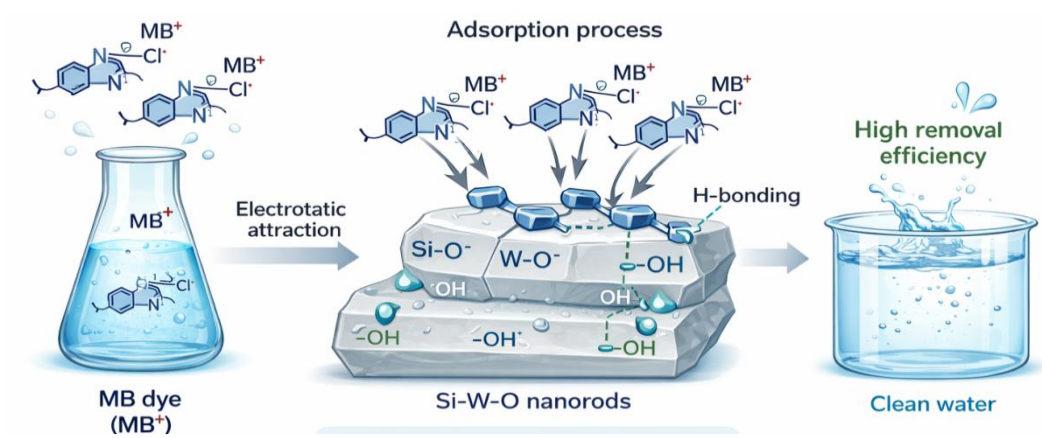

1 INTRODUCTION

Nanomaterials have attracted considerable scientific and technological interest over the past two decades owing to their unique physicochemical properties arising from their nanoscale dimensions. From a manufacturing engineering perspective, controlled material processing enables the development of functional nanostructures with tailored morphology, surface chemistry, and performance characteristics. Their high surface-area-to-volume ratio, abundant active sites, and tunable surface functionality enable their integration into engineered material systems for applications including energy storage [1], biomedical engineering [2], environmental remediation, and sensing technologies. In particular, the incorporation of nanomaterials into composite structures for water purification systems has emerged as a promising approach to address global challenges related to water contamination and environmental sustainability [3–5].

Among various water pollutants, synthetic dyes represent one of the most serious environmental challenges because of their widespread industrial use, high chemical stability, and resistance to biodegradation. Methylene blue (MB) [6], a cationic dye extensively employed in textile, leather, pharmaceutical, and printing industries, is commonly selected as a model pollutant for evaluating adsorption performance owing to its high solubility and persistence in aqueous media [7]. The excessive discharge of MB into aquatic systems poses serious environmental and health risks, necessitating the development of engineered material solutions for efficient removal. MB contamination can reduce light penetration in water bodies, thereby affecting photosynthetic activity and disrupting aquatic ecosystems [8,9]. Moreover, recent advances in nanotechnology have enabled the development of highly sensitive nanosensing platforms for monitoring water quality and detecting various waterborne contaminants [10]. Also, prolonged exposure to MB has been associated with toxicological effects in humans and aquatic organisms. Consequently, the efficient removal of MB dye from wastewater has become a critical environmental priority.

Numerous conventional wastewater treatment technologies, including coagulation, flocculation, filtration, and biological degradation, have been developed for dye removal. Nevertheless, these techniques frequently suffer from limited removal efficiency, secondary pollution, and relatively high operational expenses, particularly for chemically stable dyes such as methylene blue. Consequently, nanostructured adsorbents have emerged as promising alternatives because of their high surface area, abundant active sites, and superior adsorption performance. Nanomaterials such as metal oxides [11], carbon-based nanostructures [12,13], metal–organic frameworks [14], and magnetic nanoparticles have demonstrated exceptional performance in dye removal through adsorption, photocatalysis, and advanced oxidation processes.

The effectiveness of nanomaterials in MB removal is also attributed to strong electrostatic interactions between their surfaces and dye molecules. From a composite materials design perspective, these properties can be further optimized through controlled processing techniques such as surface functionalization [15], doping, and phase integration within hybrid material systems. The incorporation of metal ions or heteroatoms can improve electron-transfer properties, thereby enhancing photocatalytic or electrochemical degradation mechanisms. These material engineering strategies not only increase removal efficiency but also improve structural integrity, durability, and reusability, which are critical factors in scalable manufacturing and industrial wastewater treatment applications.

The integration of nanomaterials into advanced engineered systems and composite-based filtration structures offers a sustainable and efficient solution for removing dye pollutants and improving water quality [16]. The development of multifunctional composite materials capable of simultaneous adsorption, degradation, and sensing of pollutants represents an emerging research direction in environmental and manufacturing engineering. Continued research focusing on scalability, process optimization, environmental safety, and regeneration capability is essential to ensure successful industrial implementation.

The hydrothermal synthesis method is a widely utilized processing technique for the fabrication of nanomaterials and nanostructured composites due to its simplicity, high efficiency, and ability to produce materials with controlled morphology and crystallinity [17,18]. From a manufacturing process perspective, hydrothermal synthesis enables precise control over microstructure development, which directly influences material performance. This method involves chemical reactions carried out in aqueous solutions under elevated temperature and pressure conditions within a sealed autoclave reactor. The hydrothermal environment facilitates dissolution, nucleation, and crystal growth, allowing control over particle size, shape, and structural properties. By adjusting process parameters such as temperature, reaction time, pH, precursor concentration, and solvent composition, materials with tailored physicochemical properties can be produced. This technique is particularly suitable for synthesizing composite systems based on metal oxides, metal sulfides, carbon-based nanomaterials, and metal–organic frameworks with high purity and uniform particle distribution.

In addition to its versatility, hydrothermal synthesis offers environmental and economic advantages compared with conventional high-temperature solid-state manufacturing methods [19]. The process operates at relatively low temperatures, reducing energy consumption and minimizing unwanted byproducts. Furthermore, the aqueous medium supports environmentally friendly processing, aligning with sustainable manufacturing principles. The method also enhances crystallinity and structural stability, which are essential for improving material performance in applications such as catalysis, adsorption, sensing, and energy storage. Although tungsten oxide (WO_3)-based adsorbents have demonstrated excellent adsorption performance owing to their surface-active oxygen species, their adsorption efficiency is often limited by particle agglomeration and restricted surface accessibility. Similarly, silica-based adsorbents have a high surface area and are chemically stable, but they generally have a lower ability to adsorb cationic dyes unless their surfaces are modified. The novelty of the present work lies in the hydrothermal manufacturing of Si–W–O nanorods that integrate the advantages of silica and tungsten oxide within a single nanostructured framework. The developed manufacturing route provides controlled morphology and oxygen-containing surface groups that may contribute to adsorption, while offering a simple, scalable, and environmentally friendly approach for methylene blue removal from aqueous solution.

In the present study, hydrothermally manufactured Si–W–O nanorods were systematically characterized to investigate the influence of the manufacturing process on their structural characteristics and adsorption performance toward methylene blue. Particular emphasis was placed on establishing the manufacturing–structure–performance relationship that governs the adsorption behavior of the Si–W–O nanorods.

2 Experimental

Hydrothermal Manufacturing of Si–W–O Nanorods

Si–W–O nanorods were hydrothermally manufactured through the following three sequential steps:

i) Twenty-five grams of yellow sand were thoroughly washed several times, dried overnight at 60 °C, and subsequently subjected to ball milling. Specifically, the dried sand was placed in a steel milling vial containing 113 g of steel balls and 50 mL of deionized water. Continuous milling was performed at 400 rpm for 8 hours.

ii) The tungstic acid precursor was prepared by passing a 0.5 M Na_2WO_4 solution through a glass column packed with 30 mL of cation-exchange resin.

iii) The transparent, yellowish ion-exchanged tungstic acid precursor was mixed with the pre-treated sand, and the resulting suspension was transferred into a Teflon-lined stainless-steel autoclave with a filling ratio of approximately 70–80%. The precursor suspension was naturally acidic owing to the formation of tungstic acid during the ion-exchange process. The sealed autoclave was hydrothermally processed at 120 °C for 24 h and subsequently allowed to cool naturally to room temperature.

3 Characterization

The crystallographic structure of the hydrothermally manufactured Si–W–O nanorods was examined using powder X-ray diffraction (XRD, Shimadzu 7000, USA, Cu-Kα radiation). Surface morphology was characterized using scanning electron microscopy (SEM, JSM-6360LA, Japan), while Fouriertransform infrared spectroscopy (FTIR, Shimadzu 8400S, Japan) was employed to identify the surface functional groups involved in the adsorption process.

4 Adsorption studies

Batch adsorption experiments were carried out in 50 mL conical flasks containing 10 mL of methylene blue (MB) solution under continuous stirring. Unless otherwise stated, 50 mg of the hydrothermally manufactured Si–W–O nanorods was used as the adsorbent. To investigate the effect of adsorbent dosage, the mass was varied from 10 to 50 mg while all other experimental parameters were maintained constant. The effects of contact time, initial dye concentration, solution pH, ionic strength, and temperature were investigated individually by varying one parameter at a time while maintaining all remaining conditions unchanged. The dye removal percentage (R%) was calculated using the following equation [20]:

$$\%R = \frac{C_o - C_e}{C_o} \times 100 \qquad (1)$$

where C_0 and C_e denote the initial and equilibrium concentrations of methylene blue in the aqueous solution (mg L^{-1}), respectively.

5 Results

Structural analysis

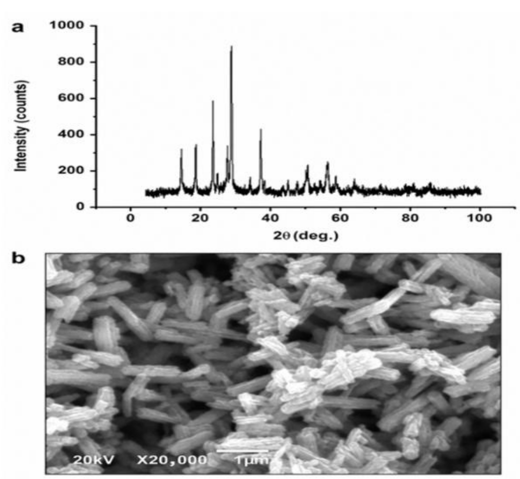

Figure 1. (a) XRD pattern and (b) SEM micrograph of the prepared Si–W–O nanorods.

The structural characteristics of the hydrothermally manufactured Si–W–O nanorods were investigated using X-ray diffraction (XRD) and scanning electron microscopy (SEM), as presented in Figure 1. The XRD pattern (Figure 1a) confirms the formation of a crystalline structure, with the majority of the diffraction peaks corresponding to the orthorhombic $WO_3 \cdot 0.33H_2O$ phase (ICDD No. 01-072-0199). SEM analysis (Figure 1b) reveals the successful formation of a rod-like morphology, indicating that the hydrothermal manufacturing process effectively controlled the growth of the Si–W–O nanorods.

Batch adsorption study

The adsorption performance of the hydrothermally manufactured Si–W–O nanorods toward methylene blue (MB) was systematically evaluated by investigating the influence of the main operating parameters affecting the adsorption process.

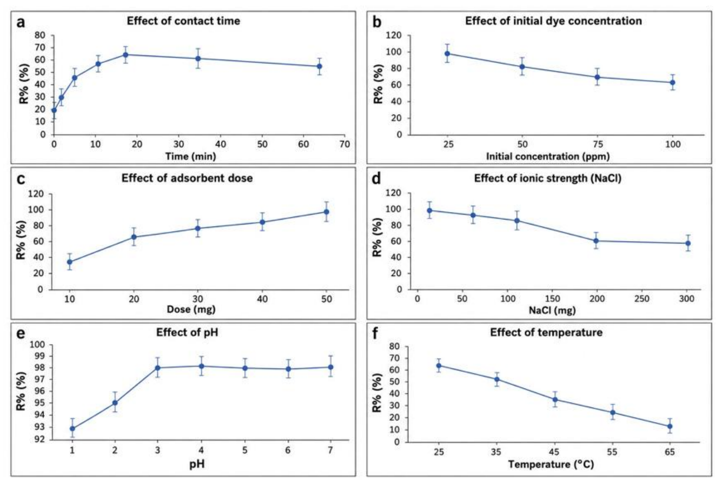

Figure 2. Adsorption performance of hydrothermally manufactured Si–W–O nanorods toward methylene blue under different operating conditions.

Unless otherwise specified, all adsorption experiments were performed using 50 mg of the hydrothermally manufactured Si–W–O nanorods. The adsorption behavior was investigated by evaluating the effects of contact time, initial dye concentration, adsorbent dosage, ionic strength, solution pH, and temperature. These experimental parameters strongly influence adsorption performance and provide valuable insights into the governing adsorption mechanism.

Figure 2a illustrates the effect of contact time on methylene blue adsorption by the hydrothermally manufactured Si–W–O nanorods. A rapid increase in removal efficiency was observed during the initial adsorption stage, reaching approximately 65–68% after 15 min owing to the availability of adsorption sites. Beyond 15 min, the adsorption process reached equilibrium, and only minor variations in removal efficiency were observed. These small fluctuations fall within the expected experimental uncertainty and may be attributed to dynamic adsorption–desorption equilibrium or normal measurement variability rather than a genuine decrease in adsorption performance. These results indicate that adsorption equilibrium was reached after approximately 15 min, which matches earlier research on nanostructured adsorbents for removing methylene blue [21].

Figure 2b presents the effect of the initial methylene blue concentration on adsorption performance. At a low dye concentration of **25 ppm**, the Si–W–O nanorods exhibit a high removal efficiency of approximately **95–100%**, demonstrating their strong adsorption capability. However, as the MB concentration increases to **50, 75, and 100 ppm**, the R% decreases to around **80%, 68%, and 63%**, respectively. The observed decrease in removal efficiency at higher dye concentrations is attributed to progressive saturation of the available adsorption sites, resulting in increased competition among dye molecules for active surface sites. These results indicate that the adsorption efficiency is concentration-dependent and favors lower pollutant loadings [22,23].

Figure 2c illustrates the effect of adsorbent dosage on the adsorption performance of methylene blue using the hydrothermally manufactured Si–W–O nanorods. Increasing the adsorbent dosage from 10 to 50 mg significantly improved the removal efficiency from approximately 35% to nearly 98%, owing to the greater availability of adsorption sites, which led to improved adsorption performance. Consequently, enhanced dye–adsorbent interactions promoted more efficient methylene blue removal. These findings demonstrate that adsorbent dosage is a key operational parameter influencing adsorption performance and that the developed Si–W–O nanorods exhibit favorable adsorption performance [24].

The impact of ionic strength, pH, and temperature on MB removal is depicted in **Figures 2d–f**. As shown in **Figure 2d**, increasing NaCl concentration from **0 to 300 mg** results in a decline in R% from approximately **95% to about 58–60%**, indicating that competing ions interfere with dye adsorption by weakening electrostatic interactions [25,26].

In **Figure 2e**, the removal efficiency increases from around **92% at pH 1** to approximately **98% in the pH range of 3–7**, suggesting that neutral to mildly alkaline conditions favor MB adsorption due to enhanced electrostatic attraction between the cationic dye molecules and the negatively charged Si–W–O nanorod surface. Finally, Figure 2f demonstrates that increasing the temperature from 25°C to 65°C causes a significant decrease in removal efficiency from approximately 65% to less than 20%. The observed decrease in adsorption efficiency with increasing temperature suggests that the adsorption process is predominantly exothermic. However, definitive confirmation requires thermodynamic analysis based on equilibrium adsorption data obtained at different temperatures, including the determination of ΔG°, ΔH°, and ΔS° [27,28].

FTIR Analysis

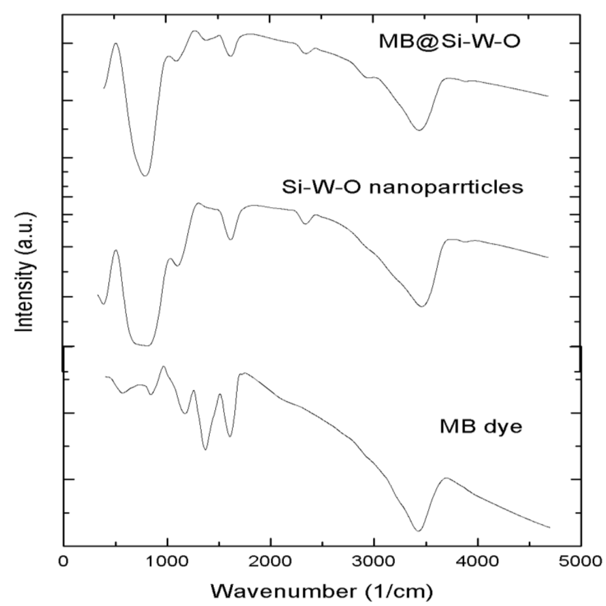

Figure 3. FTIR spectrum of MB dye, Si–W–O nanorods, and MB on Si–W–O nanorods.

Table 1. FTIR band assignments of MB dye, Si–W–O nanorods, and MB-loaded Si–W–O nanorods.

Wavenumber (cm^{-1})	Assignment	Sample
3400–3500	O–H stretching vibration of surface hydroxyl groups and adsorbed water	Si–W–O, MB@Si–W–O
~1630	H–O–H bending vibration of adsorbed water	Si–W–O, MB@Si–W–O
1600–1650	Aromatic C=C and C=N stretching vibrations	MB, MB-Si–W–O
1400–1450	C–N stretching vibration	MB, MB@Si–W–O
1000–1200	Si–O–Si and Si–O–W asymmetric stretching vibrations	Si–W–O, MB@Si–W–O
450–800	W–O–W and Si–O bending vibrations	Si–W–O, MB@Si–W–O

The FTIR spectrum of pristine methylene blue (MB) dye exhibits characteristic absorption bands associated with its aromatic heterocyclic structure and functional groups. The principal FTIR absorption bands and their corresponding assignments are summarized in the corresponding table for clarity. The bands observed in the region of ~1600–1650 cm^{-1} are attributed to C=C and C=N stretching vibrations of the aromatic rings [23], while peaks around ~1400–1450 cm^{-1} correspond to C–N stretching. The absorptions between about 1000 and 1200 cm^{-1} are related to C–S–C and C–N vibrations, which confirm the distinct molecular signature of MB [23]. In addition, a broad band appearing above ~3200 cm^{-1} can be assigned to N–H stretching vibrations and adsorbed moisture, which is commonly observed for dye molecules.

The FTIR spectrum of the Si–W–O nanorods in figure 3 shows distinct bands characteristic of metal–oxygen and silicate frameworks. The strong absorption band observed in the region of approximately 900–1100 cm^{-1} is attributed primarily to the asymmetric stretching vibrations of Si–O–Si bonds and may also indicate the presence of Si–O–W linkages, as commonly reported for silica–tungsten oxide composite systems. The formation of such linkages is consistent with the hydrothermal interaction between silica-derived species and tungsten oxide precursors during synthesis [29]. Bands observed at lower wavenumbers (~450–800 cm^{-1}) are attributed to bending vibrations of W–O–W and Si–O linkages. A broad band centered around ~3200–3500 cm^{-1}, together with a weak band near ~1630 cm^{-1}, is associated with O–H stretching and bending vibrations of surface hydroxyl groups and physically adsorbed water, which play a crucial role in adsorption processes [30].

Upon adsorption of MB dye onto the Si–W–O nanorods (MB@Si–W–O), noticeable changes in the FTIR spectrum are observed, suggesting possible interaction between the dye molecules and the adsorbent surface. Several characteristic MB peaks, particularly those corresponding to aromatic C=C/C=N (~1600 cm^{-1}) and C–N stretching vibrations, exhibit reduced intensity and slight shifts in position. Simultaneously, the Si–O–Si/Si–O–W band in the ~900–1100 cm^{-1} region shows subtle shifts and broadening, suggesting interactions between MB molecules and the inorganic framework [29]. In general, the FTIR band assignments of MB dye, Si–W–O nanorods, and MB-loaded Si–W–O nanorods can be shown in Table 1.

These spectral changes suggest that adsorption may involve interactions between MB molecules and oxygen-containing surface groups of the Si–W–O nanorods. Possible adsorption mechanisms include electrostatic attraction, hydrogen bonding, and surface complexation; however, additional surface-charge characterization is required for definitive mechanistic confirmation. The negatively charged oxygen-containing groups ($Si–O^-$ and $W–O^-$) on the Si–W–O surface can electrostatically attract the cationic MB molecules, while surface hydroxyl groups facilitate hydrogen bonding with nitrogen-containing functional groups of MB. Additionally, possible π–π interactions between the aromatic rings of MB and surface-active sites may further enhance adsorption. Overall, the FTIR results support the proposed adsorption mechanism . The effective immobilization of MB onto the Si–W–O nanorods further supports the proposed adsorption mechanism.

Adsorption Mechanism of MB Dye on Si–W–O Nanorods

The adsorption of methylene blue (MB) onto hydrothermally manufactured Si–W–O nanorods is governed by synergistic physicochemical interactions arising from the cationic nature of MB and the oxygen-rich surface of the Si–W–O framework. In aqueous media, MB predominantly exists as a positively charged species due to its quaternary ammonium group. Meanwhile, the Si–W–O nanorods possess abundant surface oxygen functionalities, including $Si–O^{-}$, $W–O^{-}$, and surface hydroxyl (–OH) groups, which become negatively charged under neutral and mildly alkaline conditions. The observed adsorption behavior is consistent with a possible contribution from electrostatic interactions between the cationic MB molecules and oxygen-containing surface groups of the Si–W–O nanorods. Nevertheless, direct confirmation of the surface charge characteristics would require zeta potential and $pH_{p}zc$ measurements, which were beyond the scope of the present study.

The observed pH dependence is consistent with this proposed mechanism. At low pH values, excessive protonation of surface oxygen sites ($Si–OH_2^{+}$) weakens electrostatic attraction, resulting in reduced adsorption efficiency. In contrast, the improved adsorption performance observed at pH 3–7 may be associated with changes in surface protonation and dye–surface interactions. However, detailed surface-charge behavior cannot be conclusively established without zeta potential or $pH_{p}zc$ measurements. This behavior is consistent with FTIR results, where noticeable shifts and intensity reductions in MB-related bands (C=C/C=N at ~1600 cm^{-1} and C–N stretching at ~1400 cm^{-1}) are observed after adsorption, suggesting interactions between MB molecules and surface oxygen groups of the Si–W–O adsorbent.

In addition to electrostatic interactions, hydrogen bonding may play a significant role in stabilizing the adsorbed MB molecules. The surface –OH groups of Si–W–O nanoparticles interact with nitrogen atoms and heterocyclic moieties of MB through hydrogen bonding. This interaction is supported by the broadening and slight shifting of the O–H stretching band (~3200–3500 cm^{-1}) in the FTIR spectrum after adsorption. Furthermore, the observed decrease in adsorption efficiency with increasing ionic strength (NaCl concentration) suggests that electrostatic interactions contribute to adsorption, as competing Na^{+} ions screen negatively charged adsorption sites and reduce MB–surface affinity.

Thermodynamic observations indicate that MB adsorption on Si–W–O nanorods is an exothermic process. The significant decrease in removal efficiency with increasing temperature suggests that the adsorption is dominated by strong surface interactions rather than diffusion-controlled processes. The rod-like morphology of Si–W–O nanorods as revealed by SEM analysis further enhances adsorption by providing a rod-like morphology and accessible surface sites, facilitating rapid initial uptake followed by equilibrium saturation. A limitation of the present work is that adsorption performance was evaluated primarily through removal efficiency (R%). Future investigations should include the determination of adsorption capacity (q_e, mg/g), together with adsorption isotherm, kinetic, and thermodynamic analyses, to enable direct comparison with previously reported adsorbent materials and provide a more comprehensive understanding of the adsorption process.

Overall, the results suggest that the adsorption mechanism may involve a combination of **electrostatic attraction**, **hydrogen bonding**, and **surface complexation**, resulting in stable immobilization of MB molecules on the Si–W–O nanorod surface. The excellent adsorption performance at low concentrations and moderate pH values demonstrate the potential of the Si–W–O nanorods for wastewater treatment applications.

Governing Adsorption Equations

Electrostatic interaction (surface complexation):

$$Si–O^{-} + MB^{+} \rightarrow Si–O^{-} \ldots MB^{+}$$

$$W–O^{-} + MB^{+} \rightarrow W–O^{-} \ldots MB^{+}$$

Comparison with Previously Reported Adsorbents for Methylene Blue Removal

To assess the adsorption performance of the hydrothermally manufactured Si–W–O nanorods, their performance was compared with that of recently reported adsorbents for methylene blue removal. As summarized in Table 2, the Si–W–O nanorods exhibit competitive removal efficiency under relatively mild operating conditions when compared with silica-based, tungsten oxide-based, and other nanostructured adsorbents reported in recent studies. Differences in adsorption performance among the reported materials may be attributed to variations in synthesis method, adsorbent dosage, initial dye concentration, contact time, solution chemistry, and the adsorption metric used (removal efficiency or adsorption capacity).

Table 2. Comparison of Si–W–O nanorods with reported adsorbents for MB removal.

Adsorbent	Adsorption performance	Experimental conditions	Reference
Hydrothermally manufactured Si–W–O nanorods (Present work)	≈95–100% removal	25 mg L^{-1} MB, 50 mg adsorbent, 10 mL solution, 15 min	Present work
Kaolinite/TiO_2 nanocomposite	92% removal	pH 7, 20 min	[31]
WO_3 nanostructures	78.14 mg g^{-1}	Batch-adsorption, pseudo-second-order kinetics	[23]
Mesoporous caged silica	≈95% removal	Rapid adsorption under ambient conditions	[32]
Silica-integrated nanocomposite	95–98% removal	pH8, rapid equilibrium	[33]

Processing–Structure–Property Relationships of Hydrothermally Synthesized Si–W–O Nanorods

From a processing–property–performance perspective, the hydrothermal synthesis conditions employed in this study played a critical role in determining the final adsorption behavior of the Si–W–O nanorods. The controlled hydrothermal environment promoted the formation of crystalline tungsten oxide domains together with a rod-like morphology, as confirmed by XRD and SEM analyses. These structural features are likely to make it easier to access active sites on the surface and help with the movement of substances during adsorption. Also, the oxygen-containing surface groups found by FTIR offer possible places for methylene blue molecules to interact. Consequently, the observed high adsorption efficiency can be attributed to the synergistic effect of the hydrothermal processing route, the resulting nanorod structure, and the surface chemical characteristics of the hydrothermally manufactured Si–W–O nanorods.

6 Conclusion

In this study, Si–W–O nanorods were successfully manufactured via a hydrothermal route and demonstrated excellent adsorption performance toward methylene blue in aqueous solution. Structural characterization confirmed the formation of crystalline rod-like Si–W–O nanorods with abundant oxygen-containing surface functional groups, which provide favorable active sites for dye adsorption. Batch adsorption experiments demonstrated that the adsorption performance was strongly influenced by the operating conditions, particularly the initial dye concentration, adsorbent dosage, pH, ionic strength, and temperature.

The reduction in adsorption efficiency at elevated ionic strength and temperature indicates that electrostatic interactions play a major role in the adsorption process and suggest predominantly exothermic adsorption behavior. Nevertheless, definitive confirmation requires thermodynamic evaluation through the determination of $\Delta G°$, $\Delta H°$, and $\Delta S°$. FTIR analysis further suggested the interaction between methylene blue molecules and the oxygen-containing surface groups of the Si–W–O nanorods through characteristic peak shifts and intensity changes. These findings support the proposed adsorption mechanism involving electrostatic attraction, hydrogen bonding, and surface complexation, which collectively promote stable immobilization of dye molecules on the adsorbent surface.

These findings demonstrate that hydrothermally manufactured Si–W–O nanorods are promising adsorbents for dye-contaminated wastewater treatment owing to their simple manufacturing process, favorable morphology, and high adsorption efficiency. Nevertheless, additional characterization using BET, EDS, XPS, zeta potential, and pH_pzc measurements would provide a more comprehensive understanding of the surface characteristics and adsorption mechanism. Future investigations should also include adsorption kinetics, equilibrium isotherms, thermodynamic analysis, adsorbent regeneration, cyclic stability, and pilot-scale evaluation to further assess the practical applicability and industrial scalability of the developed material.

References

[1] M. Hamdan, D. Abujamous, E. Abdelhafez, M. Sukkariyh, M.M. Al-Maghalseh, Parametric evaluation of sensible heat storage systems using nano-ionic liquids, J. Ecol. Eng. 26 (2025) 237–245. https://doi.org/10.12911/22998993/199322.

[2] I.M. El-Nahhal, S.M. Zourab, F.S. Kodeh, A.A. Elmanama, M. Selmane, I. Genois, F. Babonneau, Nano-structured zinc oxide-cotton fibers: Synthesis, characterization and applications, J. Mater. Sci. Mater. Electron. 24 (2013) 3970–3975. doi:10.1007/s10854-013-1349-1.

[3] A. Abu Hilal, R. Saleh, Nanotechnology Use in Water Purification for Sustainable Development of Middle East, Acad. Netw. Dev. Dialogue Pap. Ser. (2024) 121–131. doi:10.29117/andd.2022.019.

[4] M.A. Makhesana, K.M. Patel, A. Nyabadza, Applicability of nanomaterials in water and wastewater treatment: A state-of-the-art review and future perspectives, Mater. Today Proc. (2024). https://doi.org/10.1016/j.matpr.2024.01.037.

[5] E.A. Hashem, Nanotechnology in Water Treatment, Case Study : Egypt, J. Econ. Dev. Stud. 2 (2014) 243–259. doi:10.15640/jeds.v2n3a18.

[6] I. Dawood, A.H. Zyoud, S. Zyoud, A. Amireh, S.H. Zyoud, T.W. Kim, Sustainable water treatment using thermally stable natural clay: dual adsorption–thermolysis approach for organic pollutants and nitrate removal, Sci. Rep. 15 (2025) 1–13. doi:10.1038/s41598-025-12148-7.

[7] H. Sawalha, A. Bader, J. Sarsour, M. Al-Jabari, E.R. Rene, Removal of Dye (Methylene Blue) from Wastewater Using Bio-Char Derived from Agricultural Residues in Palestine: Performance and Isotherm Analysis, Processes. 10 (2022) 2039. doi:10.3390/pr10102039.

[8] M.S. Fouad, E.F. Mustafa, M.S. Hellal, M.A. Mwaheb, A comprehensive assessment of water quality in Fayoum depression, Egypt: identifying contaminants, antibiotic pollution, and adsorption treatability study for remediation, Sci. Rep. 14 (2024) 18849. doi:10.1038/s41598-024-68990-8.

[9] E. Elhaddad, A.T. Al-Fawwaz, Hormones in Aquatic Ecosystem: Problems and Solutions: Case Study in Egypt, Egypt. J. Aquat. Biol. Fish. 29 (2025) 1447–1474. doi:10.21608/ejabf.2025.429939.

[10] Z. Matar, Z.Z. Noor, A. Al-Hindi, B. Yuliarto, Recent advances in paper-based nano-biosensors for waterborne pathogen detection: Challenges and solutions, Chem. Biodivers. 22 (2025) e202403451. https://doi.org/10.1002/cbdv.202403451.

[11] S.H. Zyoud, I.S. Yahia, M. Shahwan, A.H. Zyoud, H.Y. Zahran, M.S. Abdel-wahab, M.G. Daher, M. Nasor, G.N. Makhadmeh, N. Hassan, A. Ashames, N. Qamhieh, Fast and Excellent Enhanced Photocatalytic Degradation of Methylene Blue Using Silver-Doped Zinc Oxide Submicron Structures under Blue Laser Irradiation, Crystals. 13 (2023) 229. doi:10.3390/cryst13020229.

[12] S. Sawalha, M. Assali, W. Farhoud, R. Abu-Shqair, R. Hamed, A. Qadi, Enhanced photocatalytic activity of one-pot microwave-synthesized ZnO/CND hybrid for sustainable environmental remediation, Part. Part. Syst. Charact. 42 (2025) 2400216. https://doi.org/10.1002/ppsc.202400216.

[13] M. Kamau, S. Al-Najm, M. Nandeshwar, Recent advances in carbon-based nanocomposites for environmental remediation of industrial dyes, Compos. Interfaces. 33 (2026) 567–600. doi:10.1080/09276440.2025.2534741.

[14] Z.S. Ghnim, A.H. Adhab, F.M.A. Altalbawy, M. Salih Mahdi, A. Salah Mansoor, U.K. Radi, N. Saadoun Abd, U. Abdul-Reda Hussein, H. Hussain Hamza, K. Muzammil, A. Alkhayyat, Novel pectin/chitosan Mo-MOF hydrogel for dye adsorption and pathogenic bacteria inhibition, Front. Mater. Volume 12 (2025). doi:10.3389/fmats.2025.1535825.

[15] I.M. Nassar, H. Nassar, M. Assali, M.H.S. Helal, H. Han, T.W. Kim, M. Salman, H.S. Hilal, Electro-Mineralization of Aqueous Phenazopyridine Using Platinum Nanoparticles Deposited onto Multiwalled Carbon Nanotubes, Processes. 12 (2024). doi:10.3390/pr12081625.

[16] S. Elhenawy, M. Khraisheh, F. AlMomani, M. Al-Ghouti, R. Selvaraj, A. Al-Muhtaseb, Emerging Nanomaterials for Drinking Water Purification: A New Era of Water Treatment Technology, Nanomaterials. 14 (2024) 1707. doi:10.3390/nano14211707.

[17] A.H. Zaki, S. Adel, M.M. Abd El-hafiez, A.A. Abdel-Khalek, Improved production of titanate nanotubes by hydrothermal method for adsorption of organic dyes, Beni-Suef Univ. J. Basic Appl. Sci. 10 (2021). doi:10.1186/s43088-021-00175-y.

[18] N.M. Refat, M.Y. Nassar, S.A. Sadeek, A controllable one-pot hydrothermal synthesis of spherical cobalt ferrite nanoparticles: synthesis, characterization, and optical properties, RSC Adv. 12 (2022) 25081–25095. doi:10.1039/d2ra03345c.

[19] M.M. Abady, D.M. Mohammed, T.N. Soliman, R.A. Shalaby, F.A. Sakr, Sustainable synthesis of nanomaterials using different renewable sources, Bull. Natl. Res. Cent. 49 (2025). doi:10.1186/s42269-025-01316-4.

[20] M.G. Mostafa, M.A. Sayed, Recent advances in adsorption technologies for methylene blue removal from wastewater:

Adsorbents, mechanisms, and future perspectives, Journal of Environmental Chemical Engineering. 12 (2024) 113456. https://doi.org/10.1016/j.jece.2024.113456.

[21] E.-H.A. El-Hadary, H.H. El-Feky, A. El-Qanni, I.M. Nassar, M.Y. Nassar, CdO Nanostructures: Synthesis, Characterization, and Photocatalytic Degradation of Malachite Green Dye in Aqueous Media, Asian J. Chem. Sci. 13 (2023) 24–36. doi:10.9734/ajocs/2023/v13i1230.

[22] S.K. Ahel, M.G. Munahi, Optimizing photocatalytic degradation: SnO_2–PVC thin-film catalyst for efficient removal of acridine orange, Desalin. Water Treat. 318 (2024) 100380. https://doi.org/10.1016/j.dwt.2024.100380.

[23] K. Hkiri, H.E.A. Mohamed, M.M. Abodouh, M. Maaza, Experimental and theoretical insights into the adsorption mechanism of methylene blue on the (002) WO3 surface, Scientific Reports. 14 (2024) 26991. https://doi.org/10.1038/s41598-024-78491-3.

[24] S. Sellak, J. Bensalah, H. Ouaddari, Z. Safi, A. Berisha, K. Draoui, I. Barrak, T. Guedira, M. Bourhia, S. Ibenmoussa, M. Okla, M. Dauelbait, A. Habsaoui, M. Harcharras, Adsorption of Methylene Blue Dye and Analysis of Two Clays: A Study of Kinetics, Thermodynamics, and Modeling with DFT, MD, and MC Simulations, ACS Omega. 9 (2024) 15175–15190. doi:10.1021/acsomega.3c09536.

[25] M.A. Sayed, M.G. Mostafa, Removal of Color from Textile Dyeing Effluents Using Coagulation-Flocculation Process Coupled with Adsorption on Nanoparticles Process, Jordan J. Earth Environ. Sci. 15 (2024) 287–297.

[26] A. Amjlef, S. Farsad, A. Ait El Fakir, A. El Asri, S. El Issami, S. Et-Taleb, N. El Alem, Polyaniline-encapsulated quartz sand as an adsorbent composite for Orange G dye removal from aqueous solution: Experimental and computational study, Ceram. Int. 49 (2023) 14120–14134. doi:https://doi.org/10.1016/j.ceramint.2022.12.293.

[27] A. Salahat, O. Hamed, A. Deghles, K. Azzaoui, H. Qrareya, M. Assali, W. Mansour, S. Jodeh, G.G. Hacıosmanoğlu, Z.S. Can, B. Hammouti, A.B.D. Nandiyanto, A. Ayerdi-Gotor, L. Rhazi, Olive Industry Solid Waste-Based Biosorbent: Synthesis and Application in Wastewater Purification, Polymers (Basel). 15 (2023) 1–19. doi:10.3390/polym15040797.

[28] A.Y. Al Haj Ahmed, H. Al Najar, N.A. Ghalwa, Boron adsorption from aqueous solutions using chemically activated kaolin clay adsorbents kinetics isotherm and thermodynamic studies, Sci. Rep. 15 (2025) 1–22. doi:10.1038/s41598-025-26758-8.

[29] M. S. El-Shall, V. Abdelsayed, A. Khder, H. M. A. Hassan, H. M. El-Kaderi, T. E. Reich, J. C. Chowdhury, "Nanoporous tungsten oxide/silica aerogel and xerogel catalysts: Synthesis, characterization, and catalytic activity," Journal of Physical Chemistry C, 113 (2009) 11234–11242.

[30] A.A. Aziz, H.F. Nassar, M.T. Al-Shemy, O.A. Mohamed, Boosting the mechanical performance and fire resistivity of white ordinary portland cement pastes via biogenic mesoporous silica nanoparticles, Sci. Rep. 15 (2025) 1–17. doi:10.1038/s41598-025-86798-y.

[31] Fendi, K., Bouzidi, N., Boudraa, R., Saidani, A., Manseri, A., Eliche-Quesada, D., Hai, T.N., Bollinger, J.C., Salvestrini, S., Kebir, M., Belkessa, N., Mouni, L., Testing of kaolinite/TiO_2 nanocomposites for methylene blue removal: photodegradation and mechanism, International Journal of Chemical Reactor Engineering, 22 (2025). https://doi.org/10.1515/ijcre-2024-0145.

[32] Khushnood, S., Khan, J.R., Hussain, S., Khan, H., Wahab, F., Ng, K.C., Shahzad, M.W., Synthesis and characterization of mesoporous caged silica for efficient adsorption of methylene blue from aqueous solution, Int. Commun. Heat Mass Transf. 156 (2024) 107706. https://doi.org/10.1016/j.icheatmasstransfer.2024.107706.

[33] Majeed, S., et al., Silica-Integrated Chemically Modified Human Hair Waste: A Novel Nanocomposite for Efficient Removal of Methylene Blue Dye from Water, Inorg. Chem. Commun. 172 (2025) 113747. https://doi.org/10.1016/j.inoche.2024.113747.